

# Covalent Chemistry and Conformational Dynamics of Topologically Chiral Amide-Based Molecular Knots

Oleg Lukin,<sup>[a]</sup> Walter M. Müller,<sup>[a]</sup> Ute Müller,<sup>[a]</sup> Astrid Kaufmann,<sup>[a]</sup> Claus Schmidt,<sup>[b]</sup> Jerzy Leszczynski,<sup>[c]</sup> and Fritz Vögtle\*<sup>[a]</sup>

*Dedicated to Professor J. F. Stoddart on the occasion of his 60th birthday*

**Abstract:** The readily available in gram quantities tris(allyloxy)knot of the amide-type **5** (knotane) can be completely and partially deprotected with *n*Bu<sub>3</sub>SnH in the presence of a palladium catalyst resulting in hydroxyknotanes **7–9**. These, in turn, react with diethylchlorophosphate giving rise to knotanes equipped with between one and three phosphoryl groups. Sulfonylation of bis(allyloxy)monohydroxyknotane **8** with *p*-toluenesulfonyl chloride and, following removal of one or two allyl groups from the intermediate monosulfonate **13**, give rise to sulfonyloxy-allyloxy-hydroxy- and sulfonyloxy-dihydroxy-knotanes **15** and **14**, respectively. This provides a convenient method for the preparation of knotanes with any substitution pattern. All new knotanes have

been isolated in preparative amounts and as highly pure substances with an exception of allyloxy-dihydroxyknotane **9**. This compound could only be obtained as a mixture with the corresponding monohydroxy-derivative **8**. The structures of all synthesized compounds were established by means of FAB and MALDI TOF mass spectrometry, <sup>1</sup>H and <sup>31</sup>P NMR spectroscopy. The triphosphorylated knotane **10** exhibits high solubility in alcohols, allowing its complete enantiomeric resolution with a commercially available chiral HPLC

column. <sup>1</sup>H,<sup>1</sup>H DQF-COSY correlation spectroscopy along with H/D exchange experiments and ab initio calculations provided the first detailed <sup>1</sup>H NMR signal assignments of knotanes in [D<sub>6</sub>]DMSO solution. The combination of variable temperature <sup>1</sup>H and <sup>31</sup>P NMR spectroscopy and molecular modeling has been applied to study the conformational behavior of the new knotanes in different solvents. It has been shown that in DMSO solution at room temperature knotanes exist in a relatively rigid nonsymmetrical conformation similar to that found in the solid state while faster conformational exchange leading to the average D<sub>3</sub> symmetrical structure was detected in a number of other solvents.

**Keywords:** conformation analysis • enantiomer separation • molecular knots • supramolecular chemistry • topological chirality

## Introduction

The synthesis of mechanically interlocked and intertwined molecules such as catenanes, rotaxanes and knots<sup>[1]</sup> had been

considered for a long time to be of purely theoretical interest<sup>[2]</sup> until the development of templating<sup>[3]</sup> techniques made their large-scale preparation possible. Nowadays such species are prophesied to be relevant for the construction of molecular machines<sup>[4]</sup> and fabrication of a variety of sensors and switches. They also have potential as molecular devices<sup>[5]</sup> involving large amplitude motions of mechanically-bound molecular components of catenanes or rotaxanes upon (electro)chemical or photochemical stimuli.<sup>[6–8]</sup> Despite the fact that topologically chiral molecular knots are promising units that could possibly be used in designing molecular machines<sup>[4]</sup> and remarkable achievements have been reached in their synthesis,<sup>[9–13]</sup> there are still no examples of molecular devices composed of knotted molecules. This is due to the difficulties that have been encountered during the preparative-scale synthesis, purification and especially derivatization of molecular knots. Analysis of the literature shows that beyond molecular biology techniques<sup>[1b, 9]</sup> molecular knots could be assembled: a) by metal-ion ligation of elongated phenanthrolines<sup>[10]</sup> or bipyridines;<sup>[11]</sup> b) by the interaction

[a] Prof. Dr. F. Vögtle, Dr. O. Lukin, W. M. Müller, U. Müller, M.Sc. A. Kaufmann  
Kekulé-Institut für Organische Chemie und Biochemie der Rheinischen Friedrich-Wilhelms-Universität Bonn  
Gerhard-Domagk-Strasse 1, D-53121 Bonn (Germany)  
Fax: (+49)-228-735662  
E-mail: voegtle@uni-bonn.de

[b] C. Schmidt  
Institut für Anorganische Chemie der Rheinischen Friedrich-Wilhelms-Universität Bonn  
Gerhard-Domagk-Strasse 1, D-53121 Bonn (Germany)  
Fax: (+49)-228-735327

[c] Prof. Dr. J. Leszczynski  
Computational Center for Molecular Structure and Interactions  
Department of Chemistry, Jackson State University  
Jackson, Mississippi 39217 (USA)

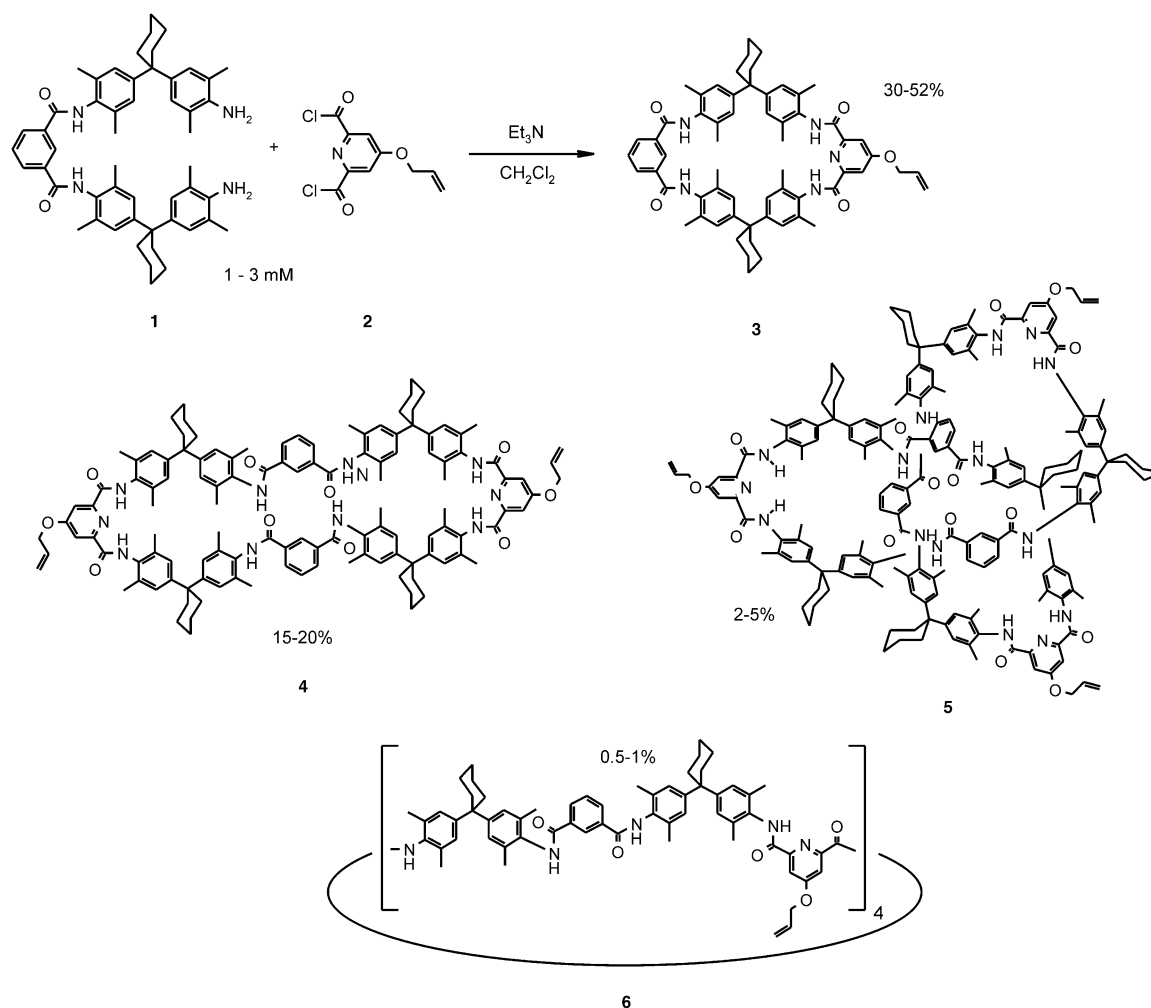
Supporting information for this article is available on the WWW under <http://www.chemeurj.org> or from the author.

between  $\pi$ -electron rich and  $\pi$ -electron deficient components of preorganized molecular chains<sup>[12]</sup> and folding assisted by intramolecular hydrogen bonding of oligoamides.<sup>[13]</sup> The latter synthesis seems attractive due to the ease of the one-pot procedure, reasonable yields and unique possibilities for further derivatizations. Recently synthesized *dendroknots*<sup>[14]</sup> containing one to three dendritic wedges on the knot periphery and a topologically chiral molecular dumbbell<sup>[15]</sup> composed of two knotanes connected by a spacer unit perfectly illustrate the synthetic potential of the amide-based molecular knots. Evidently, the development of reliable methods for laboratory scale preparation of knotted building blocks is of importance for future developments. Little is known about the conformational behavior of knotanes in solution, since only a small number of the knotane samples have to date been available for NMR studies. Investigation of the conformational properties in large molecules such as knotanes seems of great interest in view of their potential role in the construction of molecular switches where controlled conformational transitions play the key role. The present work addresses therefore the questions regarding general methods for knotane functionalization and their solvent- and temperature-dependent conformational equilibrium. Here we also explore possibilities for the construc-

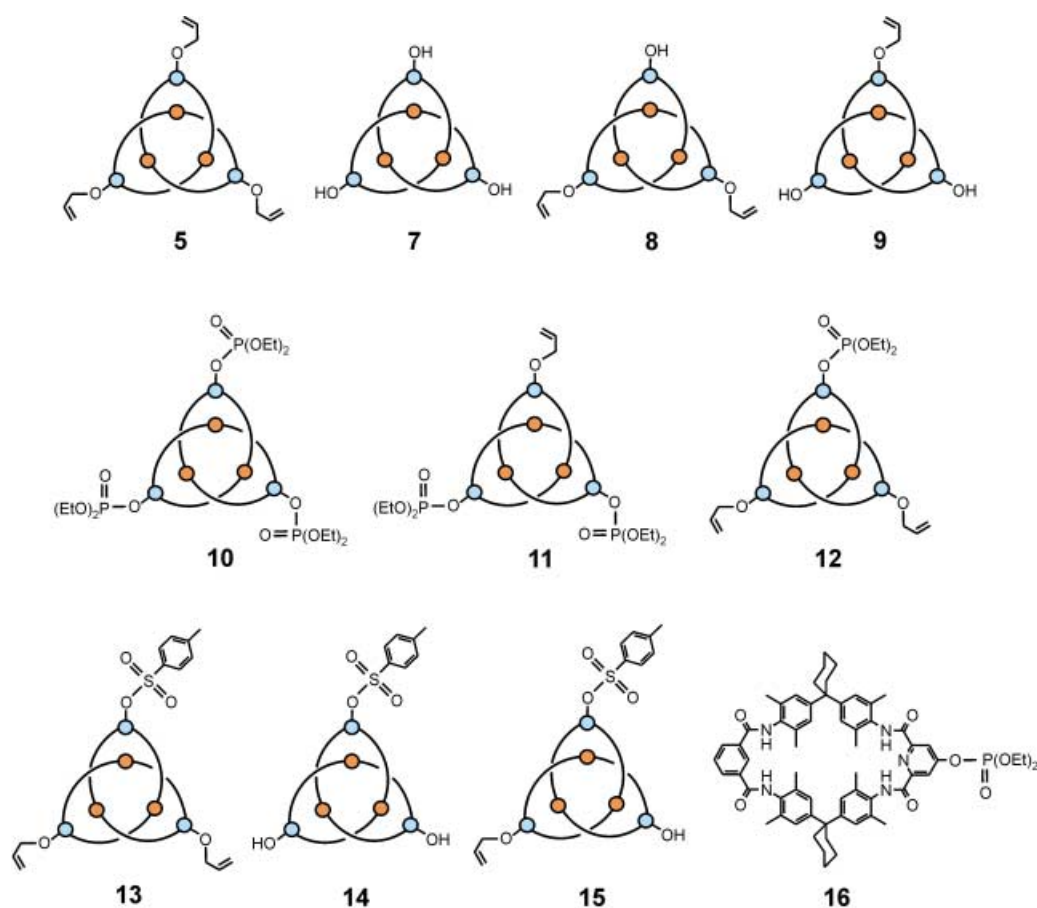
tion of knotane-based molecular devices in the foreseeable future.

## Results and Discussion

**Synthesis:** From our previous experience in knotane synthesis we thought that the yields of the amide-based knots could be increased by manipulating the kinetics of the amine acylation reaction since amide bond formation under the given conditions is irreversible. Scheme 1 illustrates the yield ranges of macrocycles **3**, **4**, and the knot **5** exerted by the variation of the reagent concentration. A 3 mM concentration of the reagents **1** and **2** provides a 5% yield of the desired knotane and has been found to be suitable for its gram scale preparation. Higher concentrations result in polymer formation. The speed of the synchronous addition of **1** and **2** has also been found to be of importance. For instance, the yields of **3–5** do not change significantly when the reagents are added in the time window of 2–17 hours, however, shortening of the reagent addition time to 0.5–1 hours gives rise to a hitherto unknown octameric macrocycle, **6** the structure of which (macromonocycle, large catenane composed of two tetramers **4** or a large knotane) remains unclear. Attempts to grow a single crystal of **6** have not been successful as yet.



Scheme 1.



Mild reduction with  $\text{Bu}_3\text{SnH}$  in the presence of 1%  $[\text{PdCl}_2(\text{PPh}_3)_2]$  allows for the complete and partial removal of the allyl groups of **5** resulting in trihydroxy- and monohydroxy-knotanes **7** and **8**, respectively.<sup>[15]</sup> We have not found satisfying conditions for the preparation of the pure dihydroxy-knot **9** because of difficulties with separation and have isolated it only as a 1:1 mixture with **8** so far.

As mentioned in the Introduction, we succeeded previously in the alkylation of a mixture of hydroxy-knotanes obtained by debenzoylation of tris(benzyloxy)knotane.<sup>[14]</sup> Only acylation with arylsulfonyl chloride could be performed with monohydroxy-knotane **8**<sup>[15]</sup> due to the intolerance of the allyl groups under the former conditions.<sup>[16]</sup> Therefore, only acylation could be used for functionalization of knotanes **8** and **9** bearing both allyl and hydroxyl groups. Introduction of biologically relevant phosphoryl groups offers great advantages in this respect since it has been shown to modify the stability, solubility and binding properties of synthetic molecular hosts such as crown ethers, cryptands, calixarenes and dendrimers.<sup>[17]</sup> It also allows for the analysis of conformation and dynamics in solution by means of <sup>31</sup>P NMR spectroscopy as exemplified by numerous studies of DNA- and protein–DNA complexes.<sup>[18]</sup> Consequently, we have introduced diethoxyphosphoryl groups by treating knotanes **7–9** with an excess of diethylchlorophosphate in the presence of triethylamine in acetone. The reaction proceeds with yields of 60–70% giving rise to tri-, di-, and monophosphorylated knotanes **10–12**. It is of note that compound **11** was synthesized from

the unseparated mixture of mono- and dihydroxy-knotanes followed by chromatographic separation of the phosphorylated products on silica gel. The phosphorylated knotanes can be converted to the parent hydroxy-derivatives after keeping them on silica gel for three days or by hydrolysis in ethanolic NaOH solution. Diethoxyphosphoryl groups have also been shown to be unstable under the conditions of the allyl group removal with  $\text{Bu}_3\text{SnH}$ . Possibilities for further knotane modifications are therefore limited. The latter difficulty can be overcome by using more chemically stable arylsulfonyl substituents. Sulfonylation of bis(allyloxy)hydroxyknotane **8** with *p*-toluenesulfonyl chloride in the presence of triethylamine in acetonitrile proceeds smoothly, giving monosulfonate **13** in 95% yield. Allyl groups, in turn, can be completely or selectively removed from the periphery of **13** (see Experimental Section) resulting in dihydroxy- and monohydroxy-knotanes **14** and **15**, respectively. The preparation of the knotanes **14** and **15** constitutes a remarkable synthetic breakthrough since knotanes bearing two hydroxyl functions (e.g. **9**) or three different substituents at the loop edges have not been isolated in the pure form previously. Thus, the sulfonylation with following allyl group splitting allows for the preparation of knotanes with any substitution pattern and opens up unique opportunities for further synthetic variations.

**Enantiomer separation:** So far all reported chiral knotane separations<sup>[13b, 14, 15]</sup> have been performed in Japan on non-

commercial Chiralpak AD HPLC columns.<sup>[19]</sup> Our efforts to use commercial chiral HPLC columns for the separation of **5** and the molecular dumbbell<sup>[15]</sup> have been unsuccessful, seemingly due to problems with solubility. Unlike its precursors, triphosphate **10** exhibits excellent solubility in almost all organic solvents, the crucial property that allowed us to carry out its complete HPLC enantiomer separation using a commercial noncovalent Chiralcel OD material.<sup>[20]</sup> A mixture of hexane/isopropanol (50:50) applied as a mobile phase showed a record-breaking separation factor  $\alpha = 4.04$  for the enantiomeric resolution of **10**. Moreover, the separations showed reasonably short retention times (less than 50 min) and have been carried out at room temperature making the whole process essentially less expensive. One milligram of each enantiomer of **10** has been collected under the latter conditions. The pronounced, mirror symmetrical circular dichroisms of the enantiomers of **10** displayed in Figure 1 confirm the purity of the compound and of the enantiomers. It should be stressed that the availability of **10** combined with its routine preparative chiral separation and the possibility of further removal of phosphoryl groups may be used in future for the synthesis of optically active knotanes which cannot be separated into enantiomers by other means.

**<sup>1</sup>H NMR signal assignments:** In order to gain insights into the solution behavior of knotanes, extensive NMR studies have been undertaken. Our previous NMR characterization of knotanes<sup>[13–15]</sup> consisted of an analytical description of the resolved signals in their proton spectra in [D<sub>6</sub>]DMSO solutions without giving assignments or discussion since on one hand only a few milligrams of the pure substances were available for the measurements, and on the other, the corresponding knotanes were shown to be less soluble.

We have now carried out a partial signal assignment of the <sup>1</sup>H NMR spectra in [D<sub>6</sub>]DMSO solution since our former investigations<sup>[13–15]</sup> revealed that, in contrast to other solvents, the [D<sub>6</sub>]DMSO proton spectra of knotanes consist of well-resolved signals at room temperature. Most of the aromatic proton signals could be assigned using <sup>1</sup>H,<sup>1</sup>H DQF-COSY experiments. Because of the similarity of the <sup>1</sup>H NMR spectra of knotanes **5**, **7** and **10** in [D<sub>6</sub>]DMSO solutions only the sample of **5** was analyzed by the DQF-COSY technique in view of its larger availability, resulting in the assignments given in Figure 2. As shown in Figure 2 most of the aromatic protons in the knotane structure are not equivalent. The most remarkable differences in chemical shifts were found for the aromatic protons of the three internal isophthaloyl diamide moieties, all of which could be discerned in the spectrum. Protons from positions 4 and 5 of two different isophthaloyl diamide rings experience the strongest shielding, making them appear at  $\delta = 5.83$  and 4.99, respectively. Protons of the iso-

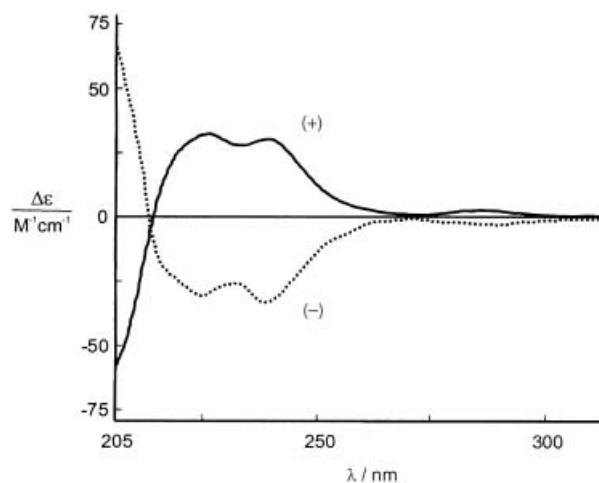


Figure 1. Circular dichroism spectra of the enantiomers of triphosphorylated knotane **10** (in methanol; concentration of each enantiomer is  $6.68 \times 10^{-5}$  M).

phthaloyl diamide rings located at positions 4 and 6 appear as pairs of different doublets. The latter observation is also supported by the signal integration in the <sup>1</sup>H NMR spectrum depicted in Figure 2. Signals pertaining to six protons of the outer 2,6-pyridindicarbamide units lie in a smaller spectral window but can still be seen as six separate signals (Figure 2). Several signals in the aromatic region show strong overlap. This is related mostly to the protons of the 2,6-dimethylaniline fragments from which 14 peaks could be found instead of the expected 24. One of these protons is substantially shifted to high field, overlapping with an olefinic multiplet at approximately  $\delta = 5.30$ . This could only be deduced from the DQF-COSY spectrum. It should also be pointed out that the latter

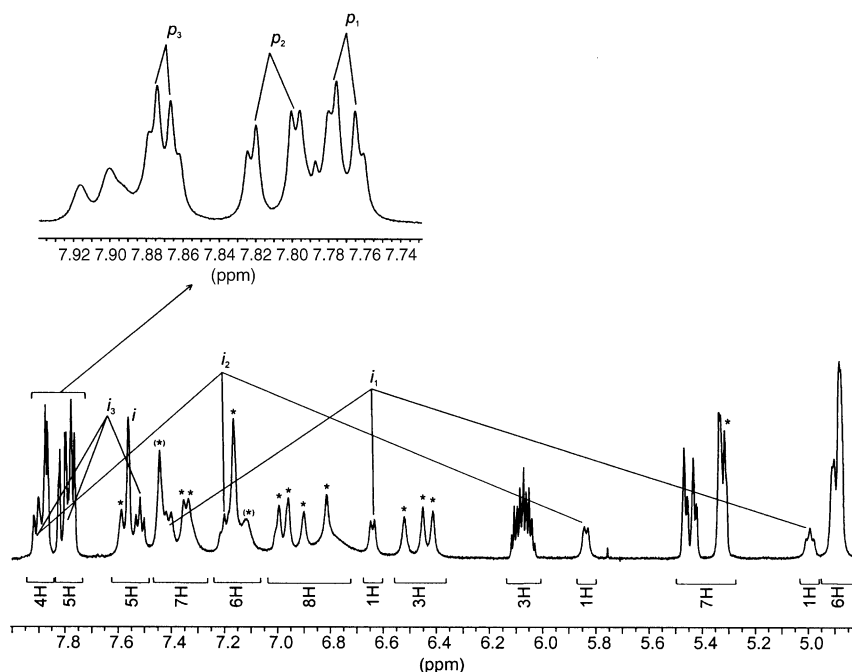


Figure 2. Signal assignments and relative integral intensities in the aromatic region of <sup>1</sup>H NMR spectrum of **5**;  $i_n$  and  $p_n$  refer to isophthaloyl diamide and 2,6-pyridinedicarbamide units, respectively. Proton signals of 2,6-dimethylaniline residues are marked with asterisks.

signal can easily be observed in the corresponding  $^1\text{H}$  NMR spectrum of **10** lacking allyl groups. Three doublets from the isophthaloyl diamide ring protons of **5** are also partially overlapped with the signals of the 2,6-pyridindicarbamide units. Some ambiguity remains in assigning the 2-isophthaloyl diamide protons. The signal at  $\delta = 7.56$  seems to be common for all three protons located at position 2 in the isophthaloyl diamide fragments since it has four cross peaks with isophthaloyl diamide doublets at  $\delta = 5.83, 6.64, 7.41$  and  $7.91$ . A good correspondence of the assigned signals with their relative integral intensities leaves no doubt about the assignment. The deficiency of equivalent protons of the knotane in its  $^1\text{H}$  NMR spectra indicates that, similar to its solid-state conformation, the knotane structure lacks symmetry and retains the relative rigidity in DMSO solution. Figure 3 schematically represents the conceivable rigid  $C_1$  knotane conformation, kinetically stable on the NMR timescale, and the  $D_3$  symmetrical average structure that could be expected assuming fast conformational transitions.

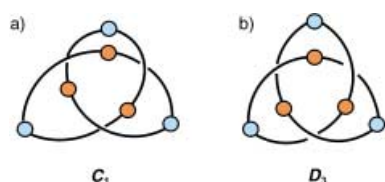


Figure 3. Cartoon representation of knotane conformations: a) rigid non-symmetrical  $C_1$ ; and b) the average  $D_3$ .

Behind the aromatic proton signals only a few other peaks can be unambiguously assigned in the knotane spectra. These include sharp multiplets pertaining to the protons of allyl and/or diethoxyphosphoryl substituents as well as three signals from the methyl groups of 2,6-dimethylaniline residues at around  $\delta = 0.06, 0.87$  and  $0.96$ . Significant shielding of the latter nuclei implies an anchored location of the corresponding groups in the interior of the knotane.

H/D exchange experiments performed for knotanes **5**, **7** and **10** in 85:15  $[\text{D}_6]\text{DMSO}/\text{CD}_3\text{OD}$  show that during 72 h twelve signals disappear in the region of  $\delta = 8.2–11.0$  revealing amide protons. Lack of equivalent amide proton signals proves additionally the nonsymmetrical and relatively robust knotane conformation in solution.

Room temperature  $^1\text{H}$  NMR spectra of the knotanes **8**, **11–14** bearing two different substituents at their 2,6-pyridindicarbamide edges show a subtle splitting of the signals that is not present in the spectra of the knotanes with three identical substituents such as **5**, **7** and **10**. The corresponding spectrum of knotane **15** owning three different peripheral groups reveals even more refined splittings. As shown in Figure 4, knotanes **5**, **7** and **10** bearing one type of the substituents on the loop edges have, as mentioned before, twelve amide proton signals while knotanes **8**, **11–12** and **15** possessing two or three different substituents exhibit considerable splitting. Assuming the stiff knotane structure, these features may originate from the different equally populated kinetically stable (in DMSO solution) knotane conformations depicted in Figure 5. Thus, for knotanes owning identical substituents

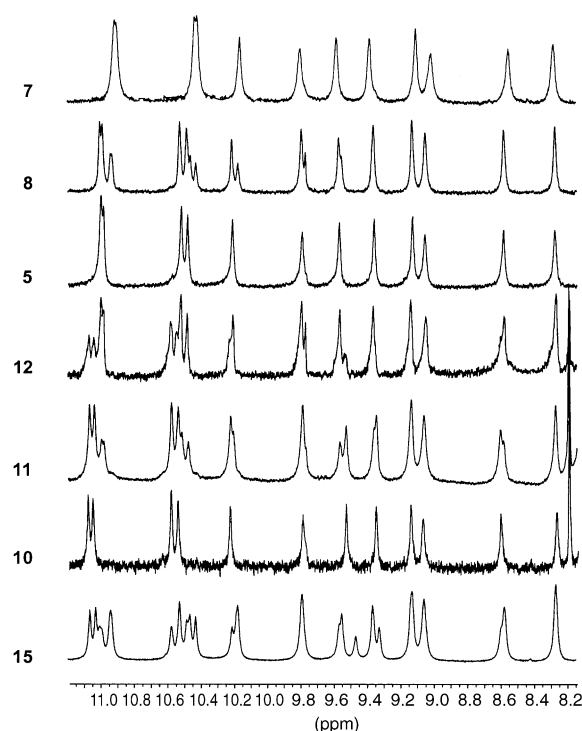


Figure 4. Amide proton regions of  $[\text{D}_6]\text{DMSO}$   $^1\text{H}$  NMR spectra of knotanes **5**, **7**, **8**, **10–12**, **15**.

( $\text{R}^1 = \text{R}^2 = \text{R}^3$ ), as in **5**, **7** and **10**, all distorted  $C_1$  configurations should be degenerate and only one could be detected by  $^1\text{H}$  NMR. Figure 5 also indicates that three different conformers can be anticipated in case of knotanes **8**, **11–12** (i.e.,  $\text{R}^1 = \text{R}^2 \neq \text{R}^3$ ) while six dissimilar combinations are possible for knotane **15** containing three different substituents ( $\text{R}^1 \neq \text{R}^2 \neq \text{R}^3$ ). The proposed model of the conformational

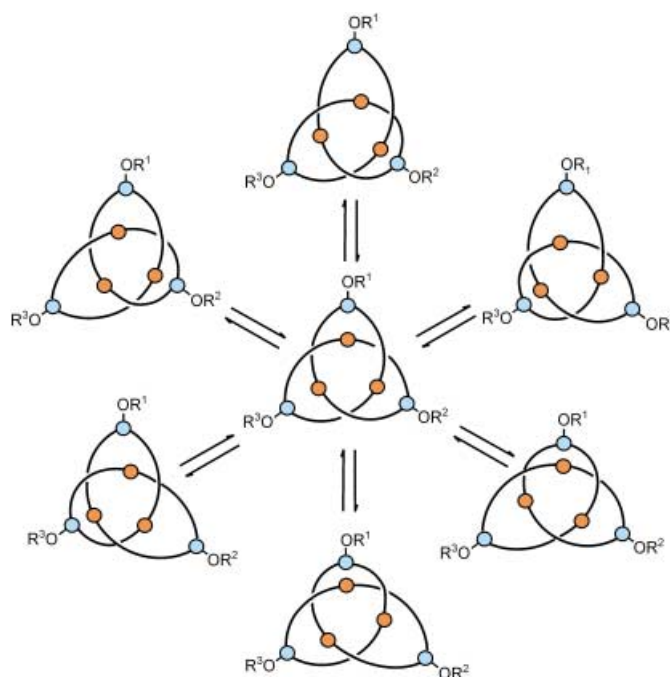


Figure 5. Schematic representation of conformational exchange in knotanes as derived from  $^1\text{H}$  NMR and  $^{31}\text{P}$  measurements.

equilibrium of knotanes in Figure 5 provides a good interpretation of the observed splitting of the peaks in the  $^1\text{H}$  NMR (Figure 4) and, as will be shown below,  $^{31}\text{P}$  NMR spectra.

Among the amide proton signals shown in Figure 4, only four low field signals show noticeable chemical shift alteration upon O-substituent exchange in 2,6-pyridindicarbamide rings. It would be reasonable to assume that these signals arise from the amide protons of the latter fragments.

On the basis of NOE measurements of amide-based macrocycles incorporating 2,6-pyridindicarbamide and isophthaloyl diamide fragments Hunter<sup>[21]</sup> has shown that amide proton signals belonging to the 2,6-pyridindicarbamide indeed appear in the lower field compared with amide protons of isophthaloyl diamide. The results obtained by ab initio calculations of the chemical shifts for model compounds carried out at the B3LYP/6-31G(d,p) level of theory (Figure 6) are in qualitative agreement with the experimental

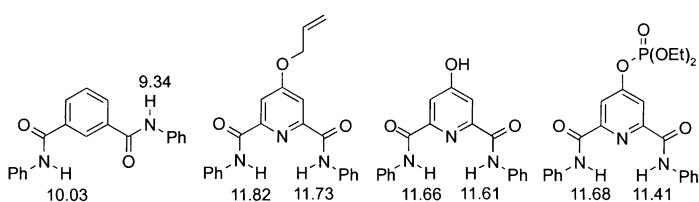


Figure 6. Amide proton chemical shifts in model compounds calculated at the B3LYP/6-31G(d, p) level of theory.

findings. Moreover, as shown in Figure 6 the calculations predict a chemical shift variation of the amide proton signals of 2,6-pyridindicarbamide upon substituent exchange. Comparison of the amide proton area in the  $^1\text{H}$  NMR spectra of **5** and **7** (Figure 4) displays, in agreement with the theory, noticeable high field shifts of 2,6-pyridindicarbamide signals in the latter knotane. Triphosphorylated knotane **10** exhibits however low field shifts of the corresponding protons (Figure 4) that contradicts the theoretical prediction depicted in Figure 6. The discrepancy between the experimental and theoretical trends can be attributed to solvent effects since the calculations have been performed for the structures in a vacuum. Use of low-polar  $\text{CDCl}_3$  instead of  $[\text{D}_6]\text{DMSO}$  shows that in model macrocycles **4** and **16** the proton signals of the controversial 4-allyloxy- and 4-phosphoryloxy-2,6-pyridindicarbamides appear at  $\delta = 8.95$  and  $8.82$ , respectively, in good accord with the calculations.

Interestingly, the H/D exchange experiments described above show that the amide protons of the 2,6-pyridindicarbamide moieties in all investigated knotanes are exchanged with deuterium in  $[\text{D}_6]\text{DMSO}/\text{CD}_3\text{OD}$  over 24 hours while it takes a longer time for the remaining protons of isophthaloyl diamides to exchange. Similar exchange experiments carried out with cyclic dimer **3** and tetramer **4** demonstrated the opposite exchange rate with isophthaloyl diamide protons disappearing first. This observation seems to indicate that similar to the solid state structure,<sup>[13a, 15]</sup> isophthaloyl diamide fragments remain hidden inside the rigid knot core also in DMSO solution whereas outer pyridindicarbamide units are freely exposed to the solvent.

**$^{31}\text{P}$  NMR spectra:** Additional evidence for the relatively rigid nonsymmetrical knotane structure (Figure 3a) in DMSO solutions comes from  $^{31}\text{P}$  NMR measurements of phosphorus-containing knotanes. The room temperature  $^{31}\text{P}$  NMR spectra of **10–12** dissolved in  $[\text{D}_6]\text{DMSO}$  exhibits three signals of equal intensity indicating the conformational rigidity of the knotane structure in solution on the NMR timescale. The fact that knotanes **10–12** give identical  $^{31}\text{P}$  NMR spectra independently of the number of phosphoryl groups on the knotane periphery is consistent with the model depicted in Figure 5, suggested on the basis of the  $^1\text{H}$  NMR of knotanes. Moreover, heating the DMSO solutions of **10–12** up to  $80^\circ\text{C}$  results in coalescence of the three signals in their  $^{31}\text{P}$  NMR spectra and reveals higher conformational mobility of the knotanes at elevated temperatures. The activation energy of approximately  $16\text{ kcal mol}^{-1}$  can be estimated on the basis of coalescence temperature<sup>[22]</sup> for the gross-process of conformational exchange in knotanes in DMSO. The latter observation proposing the equivalence of three knotane loops at higher temperatures (i.e., average  $D_3$  symmetry of the knotane skeleton) is also in line with the scheme of conformational equilibrium of knotanes illustrated in Figure 5. Notably, the  $^{31}\text{P}$  NMR spectrum of the phosphorylated macrocycle **16** shows only one signal in DMSO solution at room temperature proving that the splitting observed in room temperature  $^{31}\text{P}$  NMR spectra of **10–12** do not originate from hindered rotations of the bulky phosphoryl groups.

**Solvent and temperature effects as revealed by NMR spectroscopy and molecular modeling simulations:** The influence of the nature of the solvent on the conformational mobility of the knotanes seems to be of critical importance. As shown in Figure 7, the  $^1\text{H}$  NMR spectrum of **5** recorded in  $\text{CDCl}_3$  consists of a few broad signals and delivers no structural information, pointing merely to a slow (on the NMR timescale) conformational exchange. The spectrum of **5** recorded in  $\text{CD}_2\text{Cl}_2$  (Figure 7) is more detailed, exhibiting several resolved multiplets in the aromatic region and amide proton area while, as discussed above, the  $[\text{D}_6]\text{DMSO}$  proton spectrum of the latter knotane consists of a number of sharp signals. Cooling the  $\text{CDCl}_3$  and  $\text{CD}_2\text{Cl}_2$  solutions of **5** down to  $223\text{ K}$  results in  $^1\text{H}$  NMR spectra that are very similar to the corresponding room temperature spectrum of **5** in  $[\text{D}_6]\text{DMSO}$ . It should also be mentioned that  $^1\text{H}$  NMR spectra of the different knotanes recorded in  $[\text{D}_6]\text{DMSO}$  at elevated temperatures are not very revealing. For instance, amide proton signals disappear at  $80^\circ\text{C}$ . This is most probably due to their fast (on the NMR timescale) exchange with water present in the solvent while the rest of the spectrum, except of the signals of allyl or diethoxyphosphoryl groups, is represented by a few extremely broad lines (see Supporting Information). Thus, the  $^1\text{H}$  NMR spectra as those depicted in Figure 7 can be used as an indication of the relative rigidity of the knotane conformation in solution.

Room temperature  $^1\text{H}$  NMR spectra of **5** dissolved in  $\text{C}_6\text{D}_6$ ,  $[\text{D}_5]\text{pyridine}$  and  $[\text{D}_{18}]\text{HMPA}$  consist of a few broad lines resembling the spectrum in  $\text{CDCl}_3$  and pointing to remarkable conformational transitions slowly occurring on the NMR timescale that lead to the average  $D_3$  knotane symmetry.  $^{31}\text{P}$

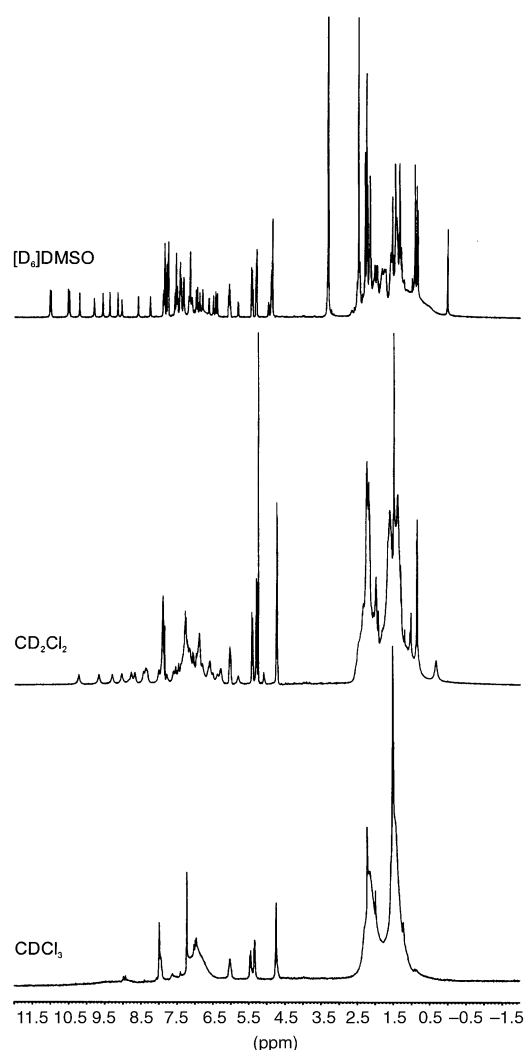


Figure 7. Room temperature 600 MHz  $^1\text{H}$  NMR spectra of **5** in  $[\text{D}_6]\text{DMSO}$ ,  $\text{CD}_2\text{Cl}_2$  and  $\text{CDCl}_3$ .

spectra of **10** in the previously mentioned solvents as well as in  $\text{CDCl}_3$  and  $\text{CD}_2\text{Cl}_2$  show only one signal, also reflecting its average  $D_3$  symmetry in these solutions.

The phosphorylated knotanes **10–12** could additionally be dissolved in  $\text{CD}_3\text{OD}$  and shown to exhibit the same very broad lines in their  $^1\text{H}$  and one signal in the corresponding  $^{31}\text{P}$  NMR spectra. Moreover, immediate exchange of the amide protons with deuterium occurring for **10–12** in pure  $\text{CD}_3\text{OD}$  reveals a noticeably high conformational freedom of the knotanes in this solvent.

Interestingly, an addition of only 10% of  $[\text{D}_6]\text{DMSO}$  to the solution of **5** in  $\text{CDCl}_3$  considerably restricts conformational motion, as reflected by the appearance of the characteristic amide proton signals and sharpening of all other signals in the  $^1\text{H}$  NMR spectrum. Similar but less remarkable spectral manifestations are observed when  $[\text{D}_6]\text{acetone}$  is added to the  $\text{CDCl}_3$  solution of **5**. The fact that the conformation of knotanes can be retained or instantly released upon the addition of solvent (i.e., by an external chemical stimulus) has much in common with the processes that puts molecular shuttles in motion.<sup>[23]</sup> Knotanes are thus thrown into the field of molecular switches.

Molecular dynamics simulations (see Experimental Section) carried out in a vacuum at 300 and 400 K show that knotanes can undergo significant local conformational transitions such as half-circle rotations of the internal isophthaloyl diamides. These transitions cause substantial distortions in the knot architecture leading to openings in the knot shell. Such an opening in the central part of the knotane can be seen in Figure 8 representing a high-energy structure snapshot taken from the 400 K molecular dynamics simulation trajectory.

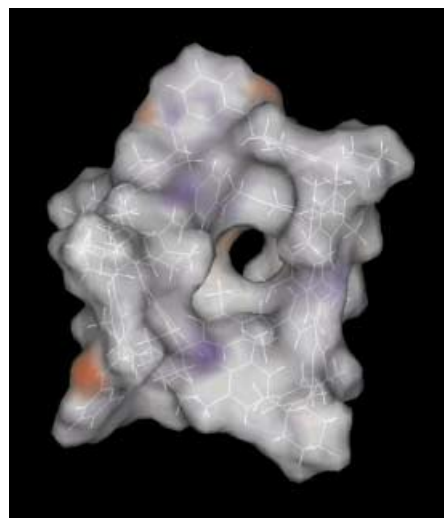


Figure 8. Solvent-accessible area of a high energy structure of a knotane. The snapshot is taken from a 400 K molecular dynamics trajectory.

Methanol molecules can easily access the internal isophthaloyl diamide protons in the latter structure, in full agreement with the experimentally observed H/D exchange described above. As follows from the molecular dynamics trajectory, the global movements in the knotane are limited to noticeable shape and size variations of the knot loops. This limitation is due to a substantial steric crowding caused mainly by outer bis(2,6-dimethylacetanilidyl)cyclohexane units prohibiting the “worm-like” dynamics in knotanes that should lead to the loop exchange observed for a demetalated phenanthroline-type knot by Sauvage et al.<sup>[24]</sup>

The fact that DMSO and acetone affect the conformation of knotanes while other polar solvents such as pyridine, HMPA and methanol show no such effect suggests that the former solvent molecules fit better within the knotane loops, forming, at the same time, hydrogen bonds to the amide protons of outer 2,6-pyridindicarbamides. Molecular mechanics calculations with an MMX force field support this suggestion showing a perfect accommodation of two DMSO molecules in the larger loops of the knotane as pictured in Figure 9. Stabilization energy of such a complex calculated from the sum of MMX total energies of the knotane and two DMSO molecules and the corresponding value of the complex is equal to  $42 \text{ kcal mol}^{-1}$ . Two acetone molecules were also shown to stabilize the complex by  $35 \text{ kcal mol}^{-1}$ . Molecular mechanics analysis of the other solvents reveals that the particle size is either too large (HMPA, pyridine, benzene,  $\text{CHCl}_3$ ) or too small ( $\text{CH}_3\text{OH}$ ) to be efficiently hosted in the

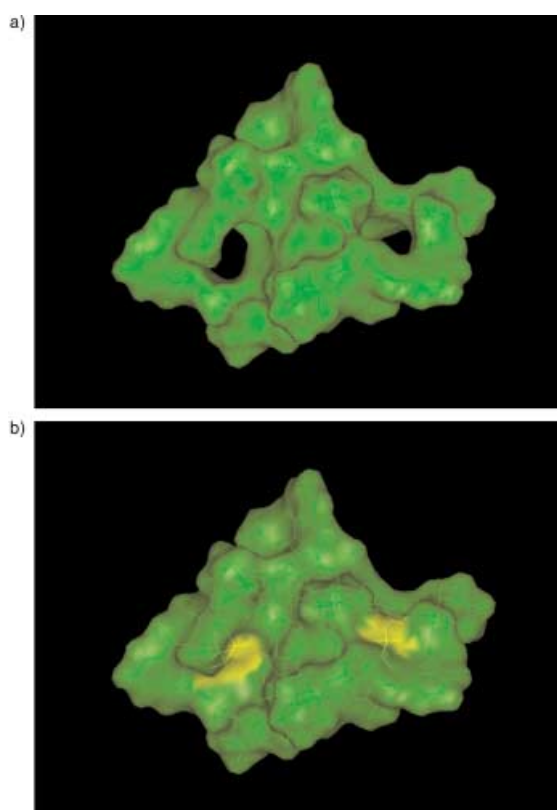


Figure 9. Solvent accessible areas a) in a minimized structure of a knotane; and b) in an energy-minimized structure of a complex composed of a knotane with two DMSO molecules located in its cavity-shaped loops.

knotane loops. Calculations also show that molecules of  $\text{CH}_2\text{Cl}_2$  exhibit a surprisingly good fit to the knotane cavities lacking, however, hydrogen bonding to the amide protons that makes this complex less stable (the corresponding stabilization energy equals to  $27 \text{ kcal mol}^{-1}$ ).

## Conclusions

New methods for the complete and partial derivatization of knotanes combining removal of outer allyl groups with phosphorylation or sulfonylation have been developed. Introduction of the biologically relevant phosphoryl groups into the knotane structure have been shown to be advantageous since the solubility is improved, expanding the possibilities for chiral separation. Moreover, phosphorus-marked knotanes can be analyzed by the means of  $^{31}\text{P}$  NMR spectroscopy, which proves to be very insightful. Partial deprotection of chemically stable monosulfonylated bis(allyloxy)knotane **13** resulted in the unique knotane bearing three different substituents at the loop edges. Complete removal of allyl groups from the monosulfonate yielded a knotane having two hydroxyl groups that could not be obtained from the parent tris(allyloxy)knotane **5** in the pure form. For the first time, signals in the  $^1\text{H}$  NMR spectra of knotanes have been interpreted on the basis of the two-dimensional  $^1\text{H}, ^1\text{H}$  DQF-COSY technique, H/D exchange experiments and ab initio calculations. The conformational behavior of the knotanes has been studied by means of  $^1\text{H}$  and  $^{31}\text{P}$  NMR spectroscopy in

different solvents. Molecular dynamics simulations carried out in a vacuum show that the rigid nonsymmetrical structure found in the solid state is retained also in DMSO solutions at room temperature while certain conformational flexibility occurs in other solvents. Moreover, the conformation of knotanes can be rigidified by the addition of small amounts of DMSO into a chloroform solution of a knotane thus exhibiting chemically-induced molecular switching which should also affect the chiroptical properties of the knotane.

On the basis of the results reported in this paper several realistic prospects can be suggested. For instance, as the X-ray and NMR results reveal, the knot looks like a three-bladed propeller with all its different blades pointing in the same direction. This is somehow reminiscent of the rotating Wankel motor central part. One can think of future unidirectional<sup>[25]</sup> movements for example after fixing chromophores at each propeller blade with following irradiating. Alternatively, enantiomerically pure, selectively monosubstituted knotanes, such as **8**, could be immobilized onto a surface (e.g. silica gel, which has been recently reported for calixarenes<sup>[26]</sup>) and set in the unidirectional motion via gas flow as theoretically proposed for an achiral molecular rotor in a box.<sup>[27]</sup>

## Experimental Section

**General remarks:** All starting materials were purchased from commercial sources or prepared using known literature procedures. The preparation of trihydroxy-knotane **7** and bis(allyloxy)hydroxy-knotane **8** has been described in our preliminary communication.<sup>[15]</sup> The solvents were dried using standard techniques. Where possible, reactions were monitored by thin-layer chromatography using DC silica gel 60F<sub>254</sub> (Merck) aluminium plates. Compounds were detected by UV light (254 nm). MPLC was done using a Büchi pump. Melting points were determined in a Reichert Thermovar microscope and are uncorrected.  $^1\text{H}$  and  $^{13}\text{C}$  NMR spectra were recorded using 300, 400, 500 and 600 MHz Bruker instruments; the solvent signals were used for internal calibration. The  $^1\text{H}-^1\text{H}$  DQF-COSY spectrum was recorded on a 500 MHz Bruker spectrometer. Mass spectra were recorded using a Concept 1H from Kratos Analytical Ltd., Manchester, GB (FAB), MALDI-TofSpec-E from MICROMASS, GB (MALDI) and Voyager-DE from PE Biosystems (MALDI).

**Chiral HPLC separations:** The enantioseparation was performed at  $25^\circ\text{C}$  on a line consisting of an analytical pump model 590 (Waters), a Rheodyne injector 7125 and a LCD2084 UV detector (Techlab). The separation was achieved on a  $10 \mu\text{m}$  semipreparative Chiralcel OD column (Daicel). The mobile phase was a mixture of hexane/isopropanol 50:50 eluting at a flow rate of  $0.5 \text{ mL min}^{-1}$ .

**Ab initio calculations:** The molecular geometries of the model substances shown in Figure 6 have been fully optimized with no symmetry restrictions using density functional theory (DFT) with B3LYP functionals.<sup>[28]</sup> Vibrational frequencies calculated for the optimized structures were found to be real. The corresponding NMR spectra have been calculated using GIAO method. The standard 6-31G(d,p) basis set was used in all calculations. Literature analysis<sup>[29]</sup> shows that the geometries, relative stabilities and frequencies of the structures calculated at this level are in a good accord with experimental data. The Gaussian<sup>[30]</sup> package of programs was used in the calculations.

**Molecular mechanics calculations and molecular dynamics simulations:** Molecular mechanics calculations were performed using the MMX force field as implemented in PCMODEL5.13.<sup>[31]</sup> Geometry optimization was accomplished with conjugate gradient procedure. A root-mean-square (rms) gradient of  $0.01 \text{ kcal mol}^{-1}$  or less was assumed as a condition of energy convergence. A value of 1.5D was assumed for the dielectric constant. The coordinates of the solid-state structure of **5** determined by single crystal X-ray analysis<sup>[15]</sup> were used to generate the initial structure



for the calculations. For the sake of simplicity the solvent found in the crystal and the allyl groups attached to 2,6-pyridinedicarbamides were moved and the resulting structure was minimized. The solvent molecules were also optimized and docked into the knotane loops followed by the energy minimization of the entire complexes. The interaction energies of the complex counterparts were estimated as the energy difference between the complex and the isolated components.

Molecular dynamics (MD) simulations were carried out using the CVFF force field as implemented in the InsightII (Discover2.9.5) program package.<sup>[32]</sup> A value of 1.5 D was assumed for the dielectric constant. The minimized structures were used as starting points for MD simulations. The structures had been equilibrated for 100 ps in all cases before the main simulations were started. The time step in all MD simulations performed was 1 fs. MD simulations were carried out at 300 and 400 K for 1 ns.

**General procedure for the synthesis of cyclic dimer 3, cyclic tetramer 4, knot (hexamer) 5, and octamer 6:** A solution of 4-allyloxy-2,6-pyridinedicarbonyl chloride (0.53 g, 2.06 mmol) in dry dichloromethane (200 mL) and a solution of *N,N'*-bis[4-[1-(4-amino-3,5-dimethyl-phenyl)cyclohexyl] 2,6-dimethyl-phenyl]isophthalamide (1.60 g, 2.06 mmol) in dry dichloromethane (200 mL) with Et<sub>3</sub>N (1.5 mL) were added simultaneously into a stirred flask containing dry dichloromethane (400 mL). After 2 h the addition was complete and the reaction mixture was stirred for a further 3 h. The solvent was removed under reduced pressure and the products were purified by chromatography on silica gel with different eluents. First CH<sub>2</sub>Cl<sub>2</sub>/acetone (20:1) was used to elute a mixture of cyclic dimer, knotane and an octamer followed by the fraction of pure tetramer. In the next step a mixture of knotane and an octamer along with pure cyclic dimer were eluted with CH<sub>2</sub>Cl<sub>2</sub>/ethyl acetate (5:1). Finally the mixture of knotane and an octamer was separated using CHCl<sub>3</sub>/ethyl acetate (5:1) as an eluent. Yields: cyclic dimer: 540 mg (29%), cyclic tetramer: 290 mg (15%), knot: 90 mg (5%), octamer: 8 mg (<1%).

**Cyclic dimer 3:** M.p. >300 °C; <sup>1</sup>H NMR (400 MHz, CDCl<sub>3</sub>): δ = 1.53 (m, 4H; CH<sub>2</sub> cyhx), 1.64 (m, 8H; CH<sub>2</sub> cyhx), 2.20 (s, 24H; ArCH<sub>3</sub>), 2.30 (m, 8H; CH<sub>2</sub> cyhx), 4.79 (m, 2H; OCH<sub>2</sub>), 5.37–5.51 (m, 2H; CH<sub>2</sub>=CH), 6.07 (m, 1H; CH=CH<sub>2</sub>), 6.97 (s, 4H; ArH), 7.00 (s, 4H; ArH), 7.26 (s, 2H; NH), 7.71 (t, *J* = 7.5 Hz, 1H; ArH), 8.00 (s, 2H; ArH), 8.18 (s, 1H; ArH), 8.22 (dd, *J* = 7.5, 1.5 Hz, 2H; ArH), 8.95 (s, 2H; NH); FAB MS: *m/z*: calcd for C<sub>62</sub>H<sub>67</sub>N<sub>5</sub>O<sub>3</sub>: 962.2; found: 962.5 [*M*<sup>+</sup>].

**Cyclic tetramer 4:** M.p. >300 °C; <sup>1</sup>H NMR (400 MHz, [D<sub>6</sub>]DMSO): δ = 1.54 (br, 24H; CH<sub>2</sub>), 2.05 (s, 24H; CH<sub>3</sub>), 2.16 (s, 24H; CH<sub>3</sub>), 2.22 (br, 8H; CH<sub>2</sub>), 2.40 (br, 8H; CH<sub>2</sub>), 4.40 (m, 4H; OCH<sub>2</sub>), 5.32–5.48 (m, 4H; CH<sub>2</sub>=CH), 6.08 (m, 2H; CH=CH<sub>2</sub>), 7.00 (s, 8H; ArH), 7.14 (s, 8H; ArH), 7.31 (t, *J* = 8 Hz, 2H; ArH), 7.79 (s, 4H; ArH), 7.87 (dd, *J* = 8, *J* = 1.5 Hz, 4H; ArH), 8.40 (brs, 2H; ArH), 9.61 (s, 4H; NH), 10.50 (s, 4H; NH); FAB MS: *m/z*: calcd for C<sub>124</sub>H<sub>134</sub>N<sub>10</sub>O<sub>10</sub>: 1924.5; found: 1925.0 [*M*<sup>+</sup>].

**Tris(allyloxy)knotane 5:** M.p. >300 °C. The NMR data are discussed in detail in the main text; only well resolved signals are referenced below. <sup>1</sup>H NMR (400 MHz, [D<sub>6</sub>]DMSO): δ = {0.06, 0.87, 0.96, 1.24, 1.29, 1.31, 1.33, 1.37, 1.49, 1.52, 1.54, 1.57, 1.60 (br), 1.82 (br), 1.99, 2.15, 2.19, 2.25, 2.28, 2.32} (132H; CH<sub>2</sub> cyhx and ArCH<sub>3</sub>), 4.90 (m, 6H; OCH<sub>2</sub>), 4.99 (t, *J* = 7 Hz, 1H; ArH), 5.32–5.48 (m, 6H; CH<sub>2</sub>=CH), 5.84 (d, *J* = 7 Hz, 1H; ArH), 6.08 (m, 3H; CH=CH<sub>2</sub>), {6.41, 6.45, 6.52, 6.63, 6.65, 6.81 (br), 6.90, 6.96, 6.99, 7.17, 7.20, 7.36, 7.44, 7.50, 7.52, 7.54, 7.56, 7.59, 7.76, 7.77, 7.80, 7.82, 7.86, 7.87, 7.90 (br), 7.92 (br)} (39H; ArH), {8.28, 8.58, 9.05, 9.13, 9.36, 9.57, 9.79, 10.21, 10.49, 10.52, 10.99, 11.00} (12H; NH); FAB MS: *m/z*: 2886.7 [*M*<sup>+</sup>]; MALDI TOF: *m/z*: calcd for C<sub>186</sub>H<sub>201</sub>N<sub>15</sub>O<sub>15</sub>: 2886.7; found: 2887.0 [*M*<sup>+</sup>], 2909.8 [*M*+Na<sup>+</sup>].

**Tris(diethoxyphosphoryloxy)knotane 10:** Diethylchlorophosphate (0.3 g, 1.7 mmol) was added to a stirred solution of trihydroxy-knotane 7 (40 mg, 0.015 mmol) and triethylamine (0.2 g, 2 mmol) in absolute acetone. The reaction mixture was stirred under reflux for 2 h and the solvent removed under reduced pressure. The crude product was purified by column chromatography on silica gel (CH<sub>2</sub>Cl<sub>2</sub>/ethyl acetate 3:1) to yield the title compound (27 mg, 60%). M.p. 220 °C; <sup>1</sup>H NMR (400 MHz, [D<sub>6</sub>]DMSO): δ = 0.06, 0.86, (brs overlapped with a triplet at 0.88 (6H; ArCH<sub>3</sub>)), 0.88 (t, 18H; CH<sub>2</sub>CH<sub>3</sub>), {0.96, 1.09, 1.11, 1.13, 1.14, 1.24, 1.28, 1.29, 1.30, 1.31, 1.32, 1.34, 1.37, 1.49, 1.56, 1.57, 1.58, 1.60, 1.62, 1.64, 1.82 (br), 1.99, 2.15, 2.20 (br), 2.25, 2.29, 2.32} (CH<sub>2</sub> and ArCH<sub>3</sub>), 4.26 (m, 12H; OCH<sub>2</sub>), {4.98 (t, *J* = 7 Hz, 1H; ArH), 5.33 (s, 1H; ArH), 5.84 (d, *J* = 7 Hz, 1H; ArH), 6.43 (s, 1H; ArH), 6.46 (s, 1H; ArH), 6.51 (s, 1H; ArH), 6.64 (d, *J* = 7 Hz, 1H; ArH),

6.83, 6.90, 6.96, 7.00, 7.17, 7.20, 7.34, 7.36, 7.40, 7.43, 7.45, 7.52 (t, *J* = 7.5 Hz), 7.56, 7.58, 7.79 (d, *J* = 7.5 Hz, 1H; ArH), 7.90 (t, *J* = 7.5 Hz, 2H; ArH), 8.07, 8.09, 8.10, 8.12, 8.19}, {8.26, 8.61, 9.07, 9.14, 9.35, 9.53, 9.79, 10.22, 10.54, 10.59, 11.05, 11.08} (12H; NH); <sup>31</sup>P NMR (162 MHz, [D<sub>6</sub>]DMSO): δ = -4.72, -4.62, -4.57; <sup>31</sup>P NMR (162 MHz, CD<sub>3</sub>OD): δ = -4.75; FAB MS: *m/z*: 3174.5 [*M*<sup>+</sup>]; MALDI TOF: *m/z*: calcd for C<sub>189</sub>H<sub>216</sub>N<sub>15</sub>O<sub>24</sub>P<sub>3</sub>: 3174.8; found: 3175.3 [*M*<sup>+</sup>], 3198.3 [*M*+Na<sup>+</sup>].

**Di- and monophosphorylated knotanes 11 and 12:** Diethylchlorophosphate (0.3 g, 1.7 mmol) was added to a stirred solution of 1:1 mixture of monohydroxy- and dihydroxy-knotanes (compounds 8 and 9) (40 mg, ca. 0.015 mmol) and triethylamine (0.2 g, 2 mmol) in absolute acetone. The reaction mixture was stirred under reflux for 2 h and the solvent removed under reduced pressure. The products were purified by chromatography on silica gel (CH<sub>2</sub>Cl<sub>2</sub>/ethyl acetate 3:1).

**Bis(diethoxyphosphoryloxy)allyloxyknotane 11:** Yield 12 mg; M.p. 250 °C; <sup>1</sup>H NMR (400 MHz, [D<sub>6</sub>]DMSO): δ = 0.06 (brs, 3H; ArCH<sub>3</sub>), 0.86 (brs overlapped with multiplet at 0.88, 6H; ArCH<sub>3</sub>), 0.88 (m, 12H; CH<sub>2</sub>CH<sub>3</sub>), 0.96 (brs, 6H; ArCH<sub>3</sub>), {1.24, 1.27, 1.29, 1.30, 1.31, 1.32, 1.34, 1.37, 1.46 (br), 1.48, 1.57, 1.60 (br), 1.82 (br), 1.99, 2.15, 2.20 (br), 2.25, 2.29, 2.32} (CH<sub>2</sub> and ArCH<sub>3</sub>), 4.27 (m, 8H; OCH<sub>2</sub>), 4.89 (m, 2H; OCH<sub>2</sub>), 4.99 (t, *J* = 7 Hz, 1H; ArH), 5.32–5.48 (m, 2H; CH<sub>2</sub>=CH), 5.84 (d, *J* = 7 Hz, 1H; ArH), 6.07 (m, 1H; CH=CH<sub>2</sub>), {6.41, 6.43, 6.45, 6.51, 6.63, 6.65, 6.81, 6.82, 6.90, 6.96, 7.00, 7.04, 7.17, 7.33, 7.36, 7.39, 7.41, 7.45, 7.50, 7.52, 7.54, 7.56, 7.58, 7.76, 7.78, 7.80, 7.82, 7.87, 7.90, 7.92, 8.07, 8.09, 8.10, 8.12, 8.19} (ArH), {8.27, 8.58, 8.60, 9.06, 9.14, 9.35, 9.37, 9.53, 9.57, 9.77, 9.79, 10.21, 10.23, 10.49, 10.52, 10.54, 10.59, 10.99, 11.00, 11.05, 11.08} (NH); <sup>31</sup>P NMR (162 MHz, [D<sub>6</sub>]DMSO): δ = -4.72, -4.62, -4.57; FAB MS: *m/z*: 3078.0 [*M*<sup>+</sup>]; MALDI TOF: *m/z*: calcd for C<sub>188</sub>H<sub>211</sub>N<sub>15</sub>O<sub>21</sub>P<sub>2</sub>: 3078.7; found: 3178.2 [*M*<sup>+</sup>], 3100.5 [*M*+Na<sup>+</sup>].

**Diethoxyphosphoryloxy-bis(allyloxy)knotane 12:** Yield 10 mg; M.p. 272 °C; <sup>1</sup>H NMR (400 MHz, [D<sub>6</sub>]DMSO): δ = 0.05, 0.86 (brs overlapped with a multiplet at 0.88), 0.88 (m, 6H; CH<sub>2</sub>CH<sub>3</sub>), 0.96, 1.24, 1.27, 1.29, 1.30, 1.31, 1.32, 1.34, 1.37, 1.46 (br), 1.48, 1.57, 1.61 (br), 1.82 (br), 1.99, 2.15, 2.19, 2.25, 2.28, 2.32, 4.27 (m, 4H; POCH<sub>2</sub>), 4.89 (m, 4H; OCH<sub>2</sub>), 4.99 (t, *J* = 7 Hz, 1H; ArH), 5.32–5.48 (m, 4H; CH<sub>2</sub>=CH), 5.84 (d, *J* = 7 Hz, 1H; ArH), 6.07 (m, 2H; CH=CH<sub>2</sub>), {6.41, 6.45, 6.51, 6.63, 6.64, 6.81, 6.90, 6.96, 7.00, 7.04, 7.17, 7.33, 7.35, 7.38, 7.41, 7.44, 7.50, 7.52, 7.56, 7.76, 7.78, 7.80, 7.82, 7.87, 7.90, 7.92, 8.07, 8.09, 8.10, 8.12, 8.19} (ArH), {8.27, 8.58, 8.60, 9.06, 9.14, 9.37, 9.53, 9.57, 9.77, 9.79, 10.21, 10.23, 10.49, 10.52, 10.54, 10.59, 10.99, 11.00, 11.05, 11.08} (NH); <sup>31</sup>P NMR (162 MHz, [D<sub>6</sub>]DMSO): δ = -4.72, -4.62, -4.57; FAB MS: *m/z*: 2981.8 [*M*<sup>+</sup>]; MALDI TOF: *m/z*: calcd for C<sub>187</sub>H<sub>206</sub>N<sub>15</sub>O<sub>18</sub>P: 2982.7; found: 2981.2 [*M*<sup>+</sup>], 3004.1 [*M*+Na<sup>+</sup>].

***p*-Toluenesulfonyloxy-bis(allyloxy)knotane 13:** *p*-toluenesulfonyl chloride (8 mg, 0.042 mmol) dissolved in dry dichloromethane (2 mL) was added to a stirred suspension containing bis(allyloxy)monohydroxy-knotane 8 (60 mg, 0.021 mmol) and triethylamine (0.1 mL, 0.7 mmol) in dry acetonitrile (10 mL). The reaction mixture was stirred under reflux for 2 h and the solvent removed under reduced pressure. The crude product was purified by column chromatography on silica gel (CH<sub>2</sub>Cl<sub>2</sub>/ethyl acetate 10:1) to yield the title compound (60 mg, 95%). M.p. >300 °C; <sup>1</sup>H NMR (400 MHz, [D<sub>6</sub>]DMSO): δ = {0.05, 0.86, 0.96, 1.24, 1.36, 1.47, 1.48, 1.57, 1.60, 1.82 (br), 1.99, 2.18, 2.25, 2.26, 2.28, 2.32, 2.44} (CH<sub>2</sub> and ArCH<sub>3</sub>), 4.89 (m, 4H; OCH<sub>2</sub>), 4.99 (t, *J* = 7 Hz, 1H; ArH), 5.32–5.48 (m, 4H; CH<sub>2</sub>=CH), 5.84 (d, *J* = 7 Hz, 1H; ArH), 6.07 (m, 2H; CH=CH<sub>2</sub>), {6.41, 6.44, 6.51, 6.64, 6.81, 6.90, 6.96, 6.99, 7.16, 7.20, 7.33, 7.35, 7.44, 7.50, 7.52, 7.53, 7.54, 7.55, 7.56, 7.58, 7.76, 7.77, 7.79, 7.80, 7.81, 7.82, 7.86, 7.87, 7.88, 7.90, 7.92, 7.93, 7.94, 7.95, 7.96, 7.97, 7.98, 7.99, 8.02 (d, *J* = 8 Hz; 2H), 8.05 (d, *J* = 8 Hz; 2H)} (ArH), {8.27, 8.58, 9.05, 9.13, 9.33, 9.36, 9.47, 9.57, 9.79, 10.19, 10.21, 10.48, 10.52, 10.57, 10.99, 11.00, 11.03, 11.06} (NH); FAB MS: *m/z*: 3000.4 [*M*<sup>+</sup>]; MALDI TOF: *m/z*: calcd for C<sub>190</sub>H<sub>203</sub>N<sub>15</sub>O<sub>17</sub>S: 3000.9; found: 2999.8 [*M*<sup>+</sup>], 3022.5 [*M*+Na<sup>+</sup>].

***p*-Toluenesulfonyloxydihydroxyknotane 14:** Bu<sub>3</sub>SnH (0.3 g, 1 mmol) was added to a vigorously stirred solution of *p*-toluenesulfonyloxy-bis(allyloxy)-knotane 13 (30 mg, 0.01 mmol) and [PdCl<sub>2</sub>(PPh<sub>3</sub>)<sub>2</sub>] (1.0 mg) in wet dichloromethane (20 mL) and the reaction mixture was allowed to stir for 6 h at room temperature. The solution was evaporated to volume of 2 mL, triturated with pentane (20 mL) and the resulting precipitate was filtered through filter paper, washed with 10 mL of pentane and chromatographed on silica gel (CH<sub>2</sub>Cl<sub>2</sub>/CH<sub>3</sub>OH 10:1) to yield the title compound (23 mg, 79%). M.p. >300 °C; <sup>1</sup>H NMR (400 MHz, [D<sub>6</sub>]DMSO): δ = {0.06, 0.86, 0.95, 1.23, 1.37, 1.48, 1.56, 1.60, 1.82 (br), 1.98, 2.18, 2.24, 2.27, 2.32, 2.44}

(CH<sub>2</sub> and ArCH<sub>3</sub>), 4.99 (t, *J* = 7 Hz, 1H; ArH), 5.33 (s, 1H; ArH), [5.84 br, 6.41, 6.44, 6.51, 6.64, 6.79, 6.90, 6.95, 6.97, 7.16, 7.20, 7.32, 7.35, 7.39, 7.44, 7.50, 7.51, 7.52, 7.53, 7.54, 7.55, 7.56, 7.57, 7.59, 7.60, 7.61, 7.62, 7.63, 7.64, 7.65, 7.67, 7.71, 7.73, 7.78, 7.80, 7.82, 7.84, 7.90, 7.92, 7.94, 7.95, 7.96, 7.97, 7.98, 7.99, 8.02 (d, *J* = 8 Hz, 2H), 8.05 (d, *J* = 8 Hz, 2H)] (ArH), {8.27, 8.58, 9.06, 9.13, 9.33, 9.37, 9.47, 9.55, 9.58, 9.79, 10.18, 10.22, 10.43, 10.47, 10.53, 10.59, 10.94, 11.03, 11.06} (NH), {11.39, 11.49, 11.58} (OH); FAB MS: *m/z*: 2920.7 [*M*<sup>+</sup>]; MALDI TOF: *m/z*: calcd for C<sub>184</sub>H<sub>195</sub>N<sub>15</sub>O<sub>17</sub>S: 2920.8; found: 2920.0 [*M*<sup>+</sup>], 2942.8 [*M*+Na<sup>+</sup>].

***p*-Toluenesulfonyloxyallyloxyhydroxyknotane 15:** Bu<sub>3</sub>SnH (3 mg, 0.01 mmol) was injected with a micro syringe into a vigorously stirred solution of of *p*-toluenesulfonyloxy-bis(allyloxy)knotane **13** (50 mg, 0.017 mmol) and [PdCl<sub>2</sub>(PPh<sub>3</sub>)<sub>2</sub>] (1 mg) in wet dichloromethane (15 mL) and the reaction mixture was allowed to stir for 6 h at room temperature. The solvent was removed under reduced pressure and the crude product was purified by chromatography on silica gel (CH<sub>2</sub>Cl<sub>2</sub>/CH<sub>3</sub>OH/Et<sub>3</sub>N 20:1:0.1) yielding the starting knotane **13** (28 mg) and the title product (17 mg, 77%). M.p. > 300 °C; <sup>1</sup>H NMR (400 MHz, [D<sub>6</sub>]DMSO): δ = {0.05, 0.86, 0.96, 1.24, 1.37, 1.47, 1.48, 1.56, 1.60, 1.82 (br), 1.98, 2.18, 2.24, 2.27, 2.32, 2.44} (CH<sub>2</sub> and ArCH<sub>3</sub>), 4.89 (m, 2H; OCH<sub>2</sub>), 4.99 (t, *J* = 7 Hz, 1H; ArH), 5.32–5.48 (m, 2H; CH<sub>2</sub>=CH), 5.84 (d, *J* = 7 Hz, 1H; ArH), 6.07 (m, 1H; CH=CH<sub>2</sub>), {6.41, 6.44, 6.51, 6.64, 6.80, 6.90, 6.96, 6.98, 7.16, 7.20, 7.33, 7.35, 7.38, 7.44, 7.50, 7.52, 7.53, 7.55, 7.59, 7.63, 7.67, 7.69, 7.73, 7.77, 7.79, 7.82, 7.87, 7.90, 7.92, 7.93, 7.94, 7.95, 7.96, 7.97, 7.98, 7.99, 8.02 (d, *J* = 8 Hz, 2H), 8.05 (d, *J* = 8 Hz, 2H)] (ArH), {8.27, 8.58, 9.06, 9.13, 9.33, 9.37, 9.45, 9.55, 9.57, 9.79, 10.18, 10.21, 10.43, 10.47, 10.48, 10.53, 10.58, 10.94, 10.99, 11.00, 11.03, 11.06} (NH), {11.39, 11.49, 11.58} (OH); FAB MS: *m/z*: 2960.6 [*M*<sup>+</sup>]; MALDI TOF: *m/z*: calcd for C<sub>187</sub>H<sub>199</sub>N<sub>15</sub>O<sub>17</sub>S: 2960.8; found: 2960.0 [*M*<sup>+</sup>], 2983.0 [*M*+Na<sup>+</sup>].

## Acknowledgement

Financial assistance by the Deutsche Forschungsgemeinschaft is gratefully acknowledged (Sonderforschungsbereich 624). O.L. thanks the Alexander von Humboldt Foundation for a fellowship. In Jackson this study was supported by NSF CREST grant No. HRD-01-25 484. We would also like to express our thanks to Prof. Dr. S. D. Peyerimhoff and Mrs. S. Müller for the theoretical calculations of the hydrogen-bond patterns. Finally we are grateful to M.Sc. S. Bitter and M.Sc. S. Buschbeck for recording MALDI-TOF mass spectra and Mr. G. Pawlitzki for measuring CD spectra.

- [1] a) G. Schill, *Catenanes, Rotaxanes and Knots*, Academic Press, New York, **1971**; b) J.-P. Sauvage, C. Dietrich-Buchecker, *Molecular Catenanes, Rotaxanes and Knots, A Journey Through the World of Molecular Topology*, Wiley-VCH, Weinheim, **1999**; c) W. S. Bryant, L. A. Guzei, A. L. Rheingold, H. W. Gibson, *Org. Lett.* **1999**, *1*, 47–50; d) C. Seel, F. Vögtle, *Chem. Eur. J.* **2000**, *6*, 21–24; e) P. N. Taylor, M. J. O'Connell, L. A. McNeill, M. J. Hall, R. T. Aplin, H. L. Anderson, *Angew. Chem.* **2000**, *112*, 3598–3602; *Angew. Chem. Int. Ed.* **2000**, *39*, 3456–3460; f) P. R. Ashton, R. Ballardini, V. Balzani, A. Credi, K. R. Dress, E. Ishow, C. J. Kleverlaan, O. Kocian, J. A. Preece, N. Spencer, J. F. Stoddart, M. Venturi, S. Wenger, *Chem. Eur. J.* **2000**, *6*, 3558–3574; g) A. M. Brouwer, C. Frochot, F. G. Gatti, D. A. Leigh, L. Mottier, F. Paolucci, S. Roffia, G. W. H. Wurple, *Science* **2001**, *291*, 2124–2128.
- [2] N. van Gulick, *New J. Chem.* **1993**, *17*, 619.
- [3] a) *Templated Organic Synthesis* (Eds.: F. Diederich, P. J. Stang), VCH-Wiley, Weinheim, **2000**; b) J. K. M. Sanders, *Pure Appl. Chem.* **2000**, *72*, 2265–2274; c) L. M. Greig, D. Philp, *Chem. Soc. Rev.* **2001**, *30*, 287–302; d) N. V. Gerbeleu, V. B. Arion, J. Burgess, *Templated Synthesis of Macrocyclic Compounds*, Wiley-VCH, Weinheim **1999**; e) T. J. Hubin, D. H. Bush, *Coord. Chem. Rev.* **2000**, *200*–202, 5; f) R. Hoss, F. Vögtle, *Angew. Chem.* **1994**, *106*, 389; *Angew. Chem. Int. Ed. Engl.* **1994**, *33*, 375; g) R. Cacciapaglia, L. Mandolini, *Chem. Soc. Rev.* **1993**, *22*, 221; h) S. Anderson, H. L. Anderson, J. K. M. Sanders, *Acc. Chem. Res.* **1993**, *26*, 469; i) B. Dietrich, P. Viout, J.-M. Lehn, *Macrocyclic Chemistry: Aspects of Organic and Inorganic Supramolecular Chemistry*, VCH, Weinheim, **1992**.
- [4] a) A. R. Pease, J. Jeppesen, J. F. Stoddart, Y. Luo, C. P. Collier, J. R. Heath, *Acc. Chem. Res.* **2001**, *34*, 433–444; b) R. Ballardini, V. Balzani, A. Credi, M. Gandolfi, M. Venturi, *Acc. Chem. Res.* **2001**, *34*, 445–455; c) A. Harada, *Acc. Chem. Res.* **2001**, *34*, 456–464; d) C. A. Schalley, K. Beizai, F. Vögtle, *Acc. Chem. Res.* **2001**, *34*, 465–476; e) J.-P. Collin, C. Dietrich-Buchecker, P. Gavina, M. C. Jiménez-Molero, J.-P. Sauvage, *Acc. Chem. Res.* **2001**, *34*, 477–487; f) V. Amendola, L. Fabbrizzi, C. Mangano, P. Pallavicini, *Acc. Chem. Res.* **2001**, *34*, 488–493.
- [5] a) C. P. Collier, E. W. Wong, M. Belohradsky, F. M. Raymo, J. F. Stoddart, P. J. Kuekes, R. S. Williams, J. R. Heath, *Science* **1999**, *285*, 391–394; b) E. W. Wong, C. P. Collier, M. Belohradsky, F. M. Raymo, J. F. Stoddart, J. R. Heath, *J. Am. Chem. Soc.* **2000**, *122*, 5831–5840; c) C. P. Collier, G. Mattersteig, E. W. Wong, Y. Lou, K. Beverly, J. Sampaio, J. F. M. Raymo, J. F. Stoddart, J. R. Heath, *Science* **2000**, *289*, 1172–1175; d) C. P. Collier, E. W. Jeppesen, Y. Luo, J. Perkins, E. W. Wong, J. R. Heath, J. F. Stoddart, *J. Am. Chem. Soc.* **2001**, *123*, 12632–12641; e) R. F. Service, *Science* **2001**, *294*, 2442–2443; f) S. Y. Chia, J. G. Cao, J. F. Stoddart, J. I. Zink, *Angew. Chem.* **2001**, *113*, 2513–2517; *Angew. Chem. Int. Ed.* **2001**, *40*, 2447–2001.
- [6] a) V. Bermudez, N. Capron, T. Gase, F. Gatti, F. Kajzar, D. A. Leigh, J. Zerbetto, S. W. Zhang, *Nature* **2000**, *406*, 608–611; b) A. Livoreil, C. O. Dietrich-Buchecker, J.-P. Sauvage, *J. Am. Chem. Soc.* **1994**, *116*, 9399–9400; c) D. J. Cárdenas, A. Livoreil, J.-P. Sauvage, *J. Am. Chem. Soc.* **1996**, *118*, 11980–11981; d) F. Baumann, A. Livoreil, W. Kaim, J.-P. Sauvage, *Chem. Commun.* **1997**, 35–36; e) A. Livoreil, J.-P. Sauvage, N. Amaroli, V. Balzani, L. Flamigni, B. Ventura, *J. Am. Chem. Soc.* **1997**, *119*, 12114–12124.
- [7] a) V. Balzani, A. Credi, S. J. Langford, F. M. Raymo, J. F. Stoddart, M. Venturi, *J. Am. Chem. Soc.* **2000**, *122*, 3542–3543; b) R. A. Bissel, E. Cordova, A. E. Kaifer, J. F. Stoddart, *Nature* **1994**, *369*, 133–137.
- [8] a) F. Vögtle, W. M. Müller, U. Müller, M. Bauer, K. Rissanen, *Angew. Chem.* **1993**, *105*, 1356–1358; *Angew. Chem. Int. Ed.* **1993**, *32*, 1295–1297; b) M. Bauer, W. M. Müller, K. Rissanen, F. Vögtle, *Liebigs Ann. Chem.* **1995**, 649–657; c) A. M. Brouwer, C. Frochot, F. G. Gatti, D. A. Leigh, L. Mottier, F. Paolucci, S. Roffia, G. W. H. Wurple, *Science* **2001**, *291*, 2124–2128; d) V. Balzani, A. Credi, F. Marchioni, J. F. Stoddart, *Chem. Commun.* **2001**, 1860–1861; e) V. Balzani, A. Credi, G. Mattersteig, O. A. Matthews, F. M. Raymo, J. F. Stoddart, M. Venturi, A. J. P. White, D. J. Williams, *J. Org. Chem.* **2000**, *65*, 1924–1936; g) P. R. Ashton, R. Ballardini, V. Balzani, A. Credi, K. R. Dress, E. Ishow, C. J. Kleverlaan, O. Kocian, J. A. Preece, N. Spencer, J. F. Stoddart, M. Venturi, S. Wenger, *Chem. Eur. J.* **2000**, *6*, 3558–3574.
- [9] N. C. Seeman, *Acc. Chem. Res.* **1997**, *30*, 357–363.
- [10] a) C. Dietrich-Buchecker, J.-P. Sauvage, *Angew. Chem.* **1989**, *101*, 192–194; *Angew. Chem. Int. Ed. Engl.* **1989**, *28*, 189–192; b) R. F. Carina, C. Dietrich-Buchecker, J.-P. Sauvage, *J. Am. Chem. Soc.* **1996**, *118*, 9110–9116; c) G. Rapenne, C. Dietrich-Buchecker, J.-P. Sauvage, *J. Am. Chem. Soc.* **1999**, *121*, 994–1001; d) S. C. J. Meskers, H. P. J. M. Dekkers, G. Rapenne, J.-P. Sauvage, *Chem. Eur. J.* **2000**, *6*, 2129–2134.
- [11] H. Adams, E. Ashworth, G. A. Breault, J. Guo, C. A. Hunter, P. C. Mayers, *Nature* **2001**, *41*, 763.
- [12] P. R. Ashton, O. A. Matthews, S. Menzer, F. M. Raymo, N. Spencer, J. F. Stoddart, D. J. Williams, *Liebigs Ann. Chem.* **1997**, 2485–2494.
- [13] a) O. Safarowsky, M. Nieger, R. Fröhlich, F. Vögtle, *Angew. Chem.* **2000**, *112*, 1699–1701; *Angew. Chem. Int. Ed.* **2000**, *39*, 1616–1618; b) F. Vögtle, A. Hüntner, E. Vogel, S. Buschbeck, O. Safarowsky, J. Recker, A. Parham, M. Knott, W. M. Müller, U. Müller, Y. Okamoto, T. Kubota, W. Lindner, E. Francotte, S. Grimme, *Angew. Chem.* **2001**, *113*, 2534–2537; *Angew. Chem. Int. Ed.* **2001**, *40*, 2468–2471; c) J. Recker, F. Vögtle, *J. Incl. Phenom. Macrocycl. Chem.* **2001**, *41*, 3–5.
- [14] J. Recker, W. M. Müller, U. Müller, T. Kubota, Y. Okamoto, M. Nieger, F. Vögtle, *Chem. Eur. J.* **2002**, *8*, 4434–4442.
- [15] O. Lukin, J. Recker, A. Böhmer, W. M. Müller, T. Kubota, Y. Okamoto, M. Nieger, F. Vögtle, *Angew. Chem.* **2003**, *115*, 458–461; *Angew. Chem. Int. Ed.* **2003**, *42*, 442–445.
- [16] Cf. A. Arduini, G. Giorgi, A. Pochini, A. Secchi, F. Uguzzoli, *J. Org. Chem.* **2001**, *66*, 8302–8308.
- [17] a) A.-M. Caminade, J.-P. Majoral, *Chem. Rev.* **1994**, *94*, 1183–1213; b) V. I. Kalchenko, D. M. Rudkevich, A. Shivanyuk, V. V. Pirozhenko,

- I. F. Tsybal, L. N. Markovsky, *Zh. Obshch. Khim. (Russ.)* **1994**, *64*, 731–739 [*Chem. Abstr.* **1995**, *122*, 314652u]; c) J. Lipkowski, O. I. Kalchenko, J. Slowikowska, V. I. Kalchenko, O. Lukin, L. N. Markovsky, R. Nowakowski, *J. Phys. Org. Chem.* **1998**, *11*, 426–435; d) O. Lukin, M. O. Vysotsky, V. I. Kalchenko, *J. Phys. Org. Chem.* **2001**, *14*, 468–473; e) C. Marmillon, F. Gauffre, T. Gulik-Krzywicki, C. Loup, A. M. Caminade, J. P. Majoral, J. P. Vors, E. Rump, *Angew. Chem.* **2001**, *113*, 2696–2699; *Angew. Chem. Int. Ed.* **2001**, *40*, 2626–2629; f) J.-P. Majoral, A.-M. Caminade, V. Maraval, *Chem. Commun.* **2002**, 2929.
- [18] D. G. Gorenstein, *Chem. Rev.* **1994**, *94*, 1315–1338.
- [19] N. Enomoto, S. Furukawa, Y. Ogasawara, H. Akano, Y. Kawamura, E. Yashima, Y. Okamoto, *Anal. Chem.* **1996**, *68*, 2798–2804. (We are grateful to Prof. Y. Okamoto (Nagoya) for the cooperation.)
- [20] a) Y. Okamoto, M. Kawashima, K. Hatada, *J. Am. Chem. Soc.* **1984**, *106*, 5357–5359; b) Y. Okamoto, M. Kawashima, K. Hatada, *J. Chromatogr.* **1986**, *363*, 173–186.
- [21] C. A. Hunter, D. H. Purvis, *Angew. Chem.* **1992**, *104*, 779–782; *Angew. Chem. Int. Ed. Engl.* **1992**, *31*, 792–795.
- [22] H. S. Gutowski, C. H. Holm, *J. Chem. Phys.* **1956**, *25*, 1228–1233.
- [23] A. S. Laine, D. A. Leigh, A. Murphy, *J. Am. Chem. Soc.* **1997**, *119*, 11 092–11 093.
- [24] C. O. Dietrich-Buchecker, J.-P. Sauvage, J. P. Kintzinger, P. Maltese, C. Pascard, J. Guilhem, *New J. Chem.* **1992**, *16*, 931–942.
- [25] a) N. Koumura, R. W. J. Zijlstra, R. A. van Delden, N. Harada, B. L. Feringa, *Nature* **1999**, *401*, 6749; b) N. Koumura, E. M. Geertsema, A. Meetsma, B. L. Feringa, *J. Am. Chem. Soc.* **2000**, *122*, 12005–12006; c) N. Koumura, E. M. Geertsema, A. Meetsma, M. B. van Gelder, B. L. Feringa, *J. Am. Chem. Soc.* **2002**, *124*, 5037–5051; d) C. A. Stanier, S. J. Alderman, T. D. W. Claridge, H. L. Anderson, *Angew. Chem.* **2002**, *114*, 1847–1850; *Angew. Chem. Int. Ed.* **2002**, *41*, 1769–1772; e) J.-P. Sauvage, report at “EURESCO conference on Supramolecular Chemistry: Molecular Rods, Wires and Switches”, San-Feliu (Spain), 14–17th September 2002. Even a chiral gas like halothan could be used for chiral recognition of the propeller in order to promote unidirectional rotation.
- [26] A. Katz, P. Da Costa, A. C. P. Lam, J. M. Notestein, *Chem. Mater.* **2002**, *14*, 3364–3368.
- [27] J. Vacek, J. Michl, report at “EURESCO conference on Supramolecular Chemistry: Molecular Rods, Wires and Switches”, San-Feliu (Spain), 14–17th September 2002.
- [28] a) A. D. Becke, *J. Chem. Phys.* **1993**, *98*, 5648; b) C. Lee, W. Yang, R. G. Parr, *Phys. Rev. B* **1988**, *37*, 785–789.
- [29] a) J. Gu, J. Leszczynski, *J. Phys. Chem. A* **2000**, *104*, 7353; b) J. Gu, J. Leszczynski, *J. Phys. Chem. A*, **2000**, *104*, 6308; c) A. M. Mebel, K. Morokuma, C. M. Lin, *J. Chem. Phys.* **1995**, *103*, 7414.
- [30] *Gaussian98*, Revision A.7, M. J. Frisch, G. W. Trucks, H. B. Schlegel, G. E. Scuseria, M. A. Robb, J. R. Cheeseman, V. G. Zakrzewski, J. A. Montgomery, Jr., R. E. Stratmann, J. C. Burant, S. Dapprich, J. M. Millam, A. D. Daniels, K. N. Kudin, M. C. Strain, O. Farkas, J. Tomasi, V. Barone, M. Cossi, R. Cammi, B. Mennucci, C. Pomelli, C. Adamo, S. Clifford, J. Ochterski, G. A. Petersson, P. Y. Ayala, Q. Cui, K. Morokuma, D. K. Malick, A. D. Rabuck, K. Raghavachari, J. B. Foresman, J. Cioslowski, J. V. Ortiz, A. G. Baboul, B. B. Stefanov, G. Liu, A. Liashenko, P. Piskorz, I. Komaromi, R. Gomperts, R. L. Martin, D. J. Fox, T. Keith, M. A. Al-Laham, C. Y. Peng, A. Nanayakkara, C. Gonzalez, M. Challacombe, P. M. W. Gill, B. Johnson, W. Chen, M. W. Wong, J. L. Andres, C. Gonzalez, M. Head-Gordon, E. S. Replogle, J. A. Pople, Gaussian, Inc., Pittsburgh, PA, **1998**.
- [31] PCMODEL is distributed by Serena Software, Dr. Kevin E. Gilbert, P.O. 3076, Bloomington, IN 47402.
- [32] Discover, Version 2.9.5, May **1994**, Biosym Technologies, 9685 Scranton Road, San Diego, CA 92121–4778.

Received: January 21, 2003 [F4749]